Effect of ocean sound speed uncertainty on matched-field geoacoustic inversion

Chen-Fen Huang
Department of Marine Environmental Informatics, National Taiwan Ocean University, Taiwan 202
chenfen@mail.ntou.edu.tw

Peter Gerstoft and William S. Hodgkiss
Marine Physical Laboratory, Scripps Institution of Oceanography, La Jolla, California, USA
gerstoft@ucsd.edu, whodgkiss@ucsd.edu

Abstract: The effect of ocean sound speed uncertainty on matched-field geoacoustic inversion is investigated using data from the SW06 experiment along a nearly range-independent bathymetric track. Significant sound speed differences were observed at the source and receiving array and several environmental parameterizations were investigated for the inversion including representing the ocean sound speed at both source and receivers with empirical orthogonal function (EOF) coefficients. A genetic algorithm-based global optimization method was applied to the candidate environmental models. Then, a Bayesian inversion technique was used to quantify uncertainty in the environmental parameters for the best environmental model, which included an EOF description of the ocean sound speed.

PACS numbers: 43.30.Pc, 43.60.Pt [JL]
Date Received: September 11, 2007 **Date Accepted:** February 25, 2008

1. Introduction

Uncertainty in ocean sound speed profiles has significant impact on matched-field geoacoustic inversion.[1–4] Although the goal of inversions is to infer the geoacoustic properties of the sea floor based on acoustic field observations received on an array, uncertainty resulting from temporal and spatial variability of the ocean sound speed plays an import role in the estimation of geoacoustic parameters, especially for higher frequencies.

The purpose of this paper and a companion paper[5] is to report the geoacoustic inversion results from stationary source data obtained during the Shallow Water 2006 experiment (SW06). We focus on the parametrization of the ocean environment, while the companion paper focuses on inverting data at several ranges. However, the two papers both invert data for a source station at 1 km range from the vertical line array. This allows for a detailed discussion of the inversion method employed in the two papers.

The experimental site is on the outer continental shelf of the western North Atlantic and is located roughly 100 miles east of Atlantic City, New Jersey. During the experiment, both acoustic and oceanographic data were collected. Significant ocean sound speed variations were observed from the conductivity-temperature-depth (CTD) measurements made at the source and receiving array. To mitigate the ocean sound speed mismatch, several environmental parameterizations were investigated, including three range-independent models and two range-dependent models. Of interest is which model can better represent the geoacoustic environment sensed by the acoustic transmissions. During this experiment, the values of the geometric parameters are reasonably well known through direct measurements.

2. The experiment

On JD239, acoustic transmissions were made from a J-15 source at 30 m depth deployed from the R/V Knorr. The experimental geometry is illustrated schematically in Fig. 1(a). A 16-element 56.25 m aperture autonomous recording vertical line array (VLA) was moored at lo-

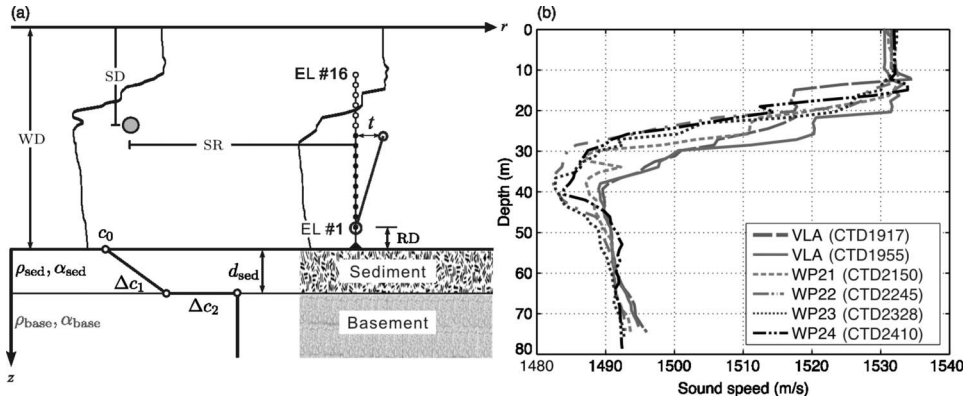

Fig. 1. Range-dependent parameterization of the SW06 environment. (b) Measured sound-speed profiles during the acoustic transmissions. The measurement time of each CTD cast is indicated as a suffix.

cation 39°1.477′N, 73°2.256′E where the water depth was 79 m. The lowermost element was 8.2 m above the bottom. Acoustic transmissions were carried out from four stations (at distances of 1, 3, 5, and 7 km from the VLA). At each station, two sets of 5 min multitonal combs were transmitted, low frequencies at 53, 103, 203 and 253 Hz, and mid frequencies at 303, 403, 503 and 703 Hz. Only the multitonal transmissions at the 1 km range (wp21; 2155-2205 universal time clock (UTC)) are discussed here.

The sound-speed profile in the water column was measured by CTD casts. Figure 1(b) shows sound-speed profiles during the acoustic transmissions. The CTD measurements at the VLA (CTD 1917 and 1955) exhibit small variations above 10 m and below 35 m. However, noticeable time-evolving sound-speed fluctuations on the order of 10 m/s are observed in the thermocline (where the sound source was located). The CTD casts were carried out at each station immediately before the start of the acoustic transmissions. Of note are the lower sound speed values in the thermocline observed in the CTDs taken at the source stations (CTD 2150, 2245, 2328 and 2410). These variations in ocean sound speed structure have an affect on the observed acoustic fields.

A geophysical survey in the study area was conducted using a high-resolution chirp sonar and GeoProbe system.[6] The chirp sonar survey, along the acoustic transmission track, showed the prominent shallow subsurface *R* reflector at 22.4 m (the *R* reflector represents an erosional surface formed during the last low stand of sea level). Preliminary GeoProbe results using the frequency band 20–50 kHz indicate that the surficial sediment sound speed is around 1620–1660 m/s near the VLA site.

3. Matched-field geoacoustic inversion

Each 5 min time series was sampled at 50 kHz and processed using 2^{17}-point fast Fourier transforms, corresponding to a snapshot of 2.6 s. The data cross-spectral density matrices (CSDMs) were computed as the average of outer products of four snapshots representing a time epoch of about 3.8 s. Due to mechanical strum contamination in the upper few array elements, only the data recorded on the lower ten elements are used.

3.1 Environmental parameterization

The base line model parameters are divided into three subsets: geoacoustic, geometrical, and ocean sound-speed parameters. Table 1 lists each environmental parameter and their search bounds. These values were selected based on *a priori* environmental knowledge.

The geoacoustic model is assumed to be range independent with a sediment layer overlying a basement, Fig. 1(a). The sediment sound speed varies linearly with depth, whereas the basement sound speed is constant. The sediment attenuation is assumed to have linear fre-

Table 1. Parameters with search bounds and Bayesian inversion results for the RD-2 model. $SAGA_{powell}$ is the best fit model using GA and the Powell method. $SAGA_{mean}$ and σ are the mean and standard deviation estimated from the Markov chain Monte Carlo derived posterior probability densities.

Model parameter		Search bounds		Inversion results	
Description	Symbol	Upper	Lower	$SAGA_{powell}$	$SAGA_{mean} \pm \sigma$
Geometric					
Source range (m)	SB	1000	1050	1040	1040 ± 3
Source depth (m)	SD	29	31	30.4	30.1 ± 0.5
Water depth at src (m)	WD_{src}	77	81	78.6	78.1 ± 0.7
Water depth at rcv (m)	WD_{rcv}	77	81	80.6	80.3 ± 0.5
1st receiver depth (m)	RD	7.5	9	8.3	8.2 ± 0.4
Array tilt (m)	t	0.5	1.5	1.15	1.08 ± 0.2
Geoacoustic					
Comp. speed (m/s)	c_0	1580	1700	1590	1596 ± 11
Incr. comp. speed (m/s)	Δc_1	0	100	20.4	23.9 ± 18
Attenuation (dB/λ)	α_{sed}	0.001	1	0.05	0.20 ± 0.2
Density (g/cm^3)	ρ_{sed}	1	2	1.8	1.7 ± 0.1
Layer thickness (m)	d_{sed}	10	30	24.2	24.7 ± 3
Incr. comp. speed (m/s)	Δc_2	50	150	129	108 ± 24
Ocean sound speed					
EOF 1_{src}/EOF 1_{rcv}		−65	−20	−65/−59	$-56 \pm 7/-52 \pm 10$
EOF 2_{src}/EOF 2_{rcv}		−25	20	−11.3/12.3	$-8.2 \pm 7/5.1 \pm 0.8$
EOF 3_{src}/EOF 3_{rcv}		−10	20	1.0/11.4	$10.0 \pm 7/7.1 \pm 8$

quency dependence, since at short range the sensitivity to nonlinear dependence is negligible. Separate simulations suggest that the inversion results are insensitive to density and attenuation in the sub-bottom. Therefore, they were set at nominal values[7] of density 2.1 g/cm^3 and attenuation 0.2 dB/λ.

The geometric parameters included in the inversions are the source range, source depth, and water depth. The array configuration is defined by estimating an effective horizontal offset between the 10th and first elements for tilt and estimating the distance of the first array element from the sea floor.

The ocean sound speed profile is parametrized by the first three EOF coefficients. Because the sound-speed difference in the thermocline layer was significant between the measured CTDs, Fig. 1(b), an empirical orthogonal function (EOF) analysis of the sound-speed measurements was carried out using all CTD measurements (16 casts) along the 80 m ISO-bath track during the period JD239 1917 to JD243 2106 UTC. Figure 2 summarizes the EOF analysis for the sound-speed profile measurements. The first three EOFs shown in Fig. 2(c) account for 95% of the variance.

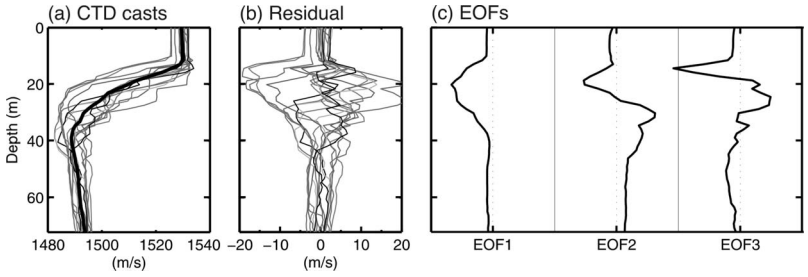

Fig. 2. EOF analysis for the SW06 CTD casts. (a) Sound-speed profiles measured from R/V Knorr and the average sound-speed profile (thick line). (b) Residual sound-speed profiles. (c) First three EOFs.

3.2 Inversion models

In the following three range-independent (RI) and two range-dependent (RD) inversion models, all five models use the same geoacoustic and geometric parameters, except for WD, as shown in Fig. 1(a) and Table 1. First, the ocean environment is assumed range independent. A typical inversion would be done using the sound speed profile corresponding to the CTD taken at the time closest to the execution of the experiment. The first model, RI-1, uses the sound speed profile measured 5 min prior to the transmission (CTD2150). The second model, RI-2, uses the sound speed profile measured at the VLA (CTD1955). The third model, RI-3, inverts for the first three EOF coefficients in order to model and estimate the sound-speed profile.

Second, a range-dependent water column is considered. The water depths at the source (WD_{src}) and VLA (WD_{rcv}) were both included in the inversion for model RD-1 and the sound-speed profiles measured at these two sites were used. In model RD-2, a total of six (three at each end) EOF coefficients were used to model the sound-speed profiles at the source and the VLA along with estimating the corresponding water depths as well.

3.3 Objective function and optimization method

The objective function measures the discrepancy between the measured acoustic and replica fields calculated for likely values of the unknown parameters. The data misfit objective function is based on the incoherent multifrequency Bartlett processor:

$$\phi(\mathbf{m}) = 1 - \frac{1}{L}\sum_{l=1}^{L} \mathbf{d}_l(\mathbf{m})^{\dagger}\mathbf{R}_l\mathbf{d}_l(\mathbf{m}), \tag{1}$$

where $\mathbf{d}(\mathbf{m})$ is the replica field generated for the vector of unknown parameters $\mathbf{m}$ normalized to have unit length, $\mathbf{R}$ is an estimated CSDM normalized to have unit trace, L the number of frequencies, and the superscript † denotes complex conjugate transpose. For the range-independent models, the normal-mode propagation code SNAP[8] was used to compute the replica fields. As for the range-dependent parameterizations, the replica fields were calculated by SNAPRD[8] based on adiabatic normal modes.

A global optimization method based on genetic algorithms (GAs) is used for the optimization. The values of the GA parameters are as follows: the population size 64; reproduction size 0.5; crossover probability 0.8; mutation probability 0.05; and the number of forward model runs for each population was 4000. For the best environmental model, the posterior probability was sampled by a Metropolis–Hastings algorithm.[8,9]

3.4 Inversion results

Matched-field geoacoustic inversion using all transmitted frequencies (eight frequencies and ten phones) was carried out for each of the above described environmental models. Table 2 tabulates the minimum values of the objective function ϕ and the water depth (WD) from the inversions. The minimum value is $SAGA_{powell}$,[8] which is found at the end of each GA run by

Table 2. Minimum values of the objective function ϕ and the parameter WD for different environmental parameterizations. For the range-dependent models, the values are for the parameters WD_{src}/WD_{rcv}.

	Range independent			Range dependent	
	RI-1	RI-2	RI-3	RD-1	RD-2
ϕ	0.301	0.212	0.196	0.304	0.187
WD	77.0	79.8	79.1	77.0 /81.0	78.6 / 80.6

carrying out a local optimization using the Powell method. Only the inversion results for the water depth are reported in the table, but a similar comparison could be made using any of the geometric parameters.

From the direct measurements, the source and VLA water depths are 79 and 78.8 m, respectively, with a standard deviation of 0.4 m. Hence, the search bound of water depth for the RI/RD cases is from 77 to 81 m. Comparing the inversion results from the range-independent models, we found that RI-1 (using the source sound speed profile) gives a rather poor inversion, the WD estimation is unreasonable (at the lower bound), and the misfit objective function has relatively high value. The inversion from RI-2 (using the VLA sound speed profile) is improved: a 30% reduction of the misfit value and the inverted WD appears near the center of the search interval. RI-3 (inverting 3 EOF coefficients) gives the best inversion results for this class. For the range-dependent models, RD-1 produces a poor inversion similar to that of RI-1. This may indicate that the source sound speed profile is not sufficiently representative of the source region of the track. RD-2 (including three sound speed EOFs and WD at both the source and VLA; an additional four more parameters than estimated in RI-3) outperforms all of the other environmental models. The smallest misfit value is achieved and an excellent agreement is obtained between the estimated and measured water depth values.

Model RD-2 is chosen for further parameter uncertainty analysis using a Markov chain Monte Carlo method based on the Metropolis–Hastings algorithm.[9] Table 1 summarizes the estimated value, $SAGA_{powell}$, and the parameter uncertainty estimate, $SAGA_{mean} \pm \sigma$, for each of the model parameters in RD-2. We see that some parameters are estimated very accurately, for example, the mean value of the upper sediment sound speed c_0 is 1596 m/s with a standard deviation of only 11.5 m/s. The inversion result is in very good agreement with the sandy bottom geoacoustic properties indicated by *in situ* measurements.[6]

The estimated sound speed profiles [Fig. 3(a)] at the source (thick dashed) and the VLA (thin dashed) are very similar to each other and resemble the measured profile at the VLA

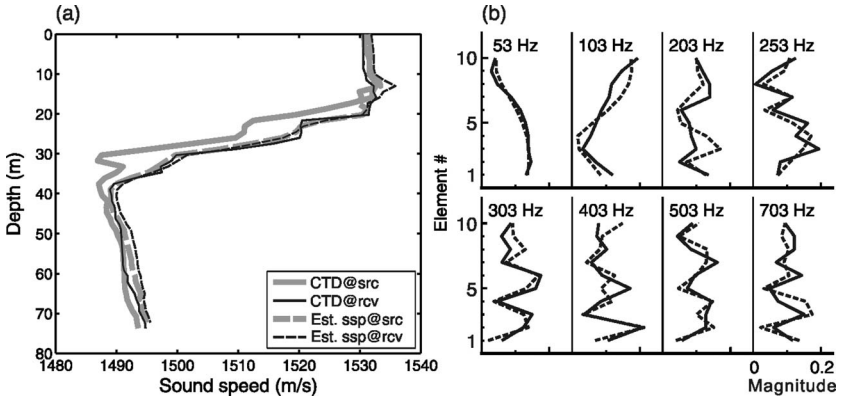

Fig. 3. Inversion results for RD-2. (a) Estimated sound speed profiles. (b) Comparison of the measured (solid) and modeled (dashed) sound fields from $SAGA_{powell}$ on the vertical array for each of the frequencies used in the inversion.

(thin solid). This might explain that the consistent misfit values obtained for both RI-3 and RD-1 models. Figure 3(b) shows good agreement between the measured (solid) and modeled (dashed) acoustic fields for the frequencies used in the inversion. At short range, it appears that the acoustic field is not particularly sensitive to the range-dependent ocean sound speed structure, and an equivalent range-independent sound speed model may be sufficient for describing the environment.

4. Discussion

The experiment took place in a very complicated ocean environment at the edge of the Gulf stream, which potentially creates strong internal waves. In a companion paper Jiang and Chapman[5] (UVic) inverts similar data along the same track with the data at 1 km range common to both papers. In the following, our paper is referred to as SIO. It is useful to discuss the difference in results, but first the two approaches are outlined:

1. Data: UVic uses one 2.6 s interval, whereas SIO uses four snapshots covering 3.8 s. More snapshots would have been beneficial.
2. UVic uses 72 2.6 s intervals (about 5 min) to estimate the data-error covariance matrix, SIO assumes a constant data error estimated from the data. This is expected to mainly influence the uncertainty analysis.
3. SIO estimates the EOFs from 16 CTD casts. However, since the sound speed profiles only vary close to the thermocline, UVic estimates the EOFs between 10 and 50 m depth and bases the estimates on just five sound speed profiles. More sound speed observations would have been preferable. This is expected to have little impact on the results.
4. Objective function (both use a Bartlett power metric), forward model (UVic uses ORCA, whereas SIO uses SNAPRD), and optimization method (both use Markov chain Monte Carlo) are not expected to result in significant differences.
5. Parameterization:

(a) Both include source range and depth, and array tilt and depth as best results are obtained if the geometric parameters are given some modest range of uncertainty.

(b) Attenuation and density are not important and will not be discussed.

(c) SIO constrains the sediment to have a positive gradient, whereas UVic also allows for negative gradients. Often marine sediments have positive gradients. In the present case, Fig. 5 of Ref. 10 from a nearby site shows cores having a negative gradient. In hindsight, the SIO sediment sound speed gradient should have been unconstrained.

(d) UVic does not allow for any ocean sound-speed range dependence. SIO allows for range dependence by inverting for ocean sound speeds at both source and VLA. This could represent an improvement if the sound speed was mildly range dependent and likely more important for the larger source ranges.

Comparing the obtained ocean bottom sound speed profile UVic obtains 1636, 1572, 1740 m/s for sediment top and bottom, and bottom half space, respectively, with a 21.1 m sediment layer. Corresponding values from SIO are 1589, 1609, and 1739 m/s with a 24 m sediment layer. Thus, the bottom half-space sound speed agrees perfectly. Based on the results of Turgut's[6] chirp profile, the sediment depth is 22.4 m, in reasonable agreement with both UVic (21.1 m) and SIO (24.2 m). The top sediment has a difference of 40 m/s between the two methods. However, the average sound speed in the sediment is probably more important for wave propagation. For this average, UVic obtains 1604 m/s, whereas SIO obtains 1599.4 m/s, also an excellent agreement. For the ocean sound speed, both obtain a sound speed profile that is similar to the measured profile at the VLA.

Uncertainty in ocean sound speed structure affects matched field geoacoustic inversion results. In the SW06 experiment, spatio-temporal variability of the ocean sound speed

structure was observed during the acoustic transmissions. The uncertainty in the ocean sound speed profiles was mitigated by including EOF coefficients for either a range-independent or range-dependent ocean sound speed environment in the inversion. The inversion results show that including sound speed EOF coefficients in the inversion yields a significantly better estimate of the geoacoustic parameters. While spatial sound speed variations were observed at the source and VLA, it was found that a single estimated sound speed profile obtained from the inversion was sufficient to represent this mildly range-dependent environment.

Acknowledgments

The SW06 was a large experiment sponsored the Office of Naval Research and involving about 50 PIs collecting both acoustic and oceanographic data. This work was supported by the Office of Naval Research Grant No. N00014-05-1-0264. In addition, C.F.H. was supported by the National Science Council and the Asian-Pacific Ocean Research Center at National Sun Yat-sen University sponsored by the Ministry of Education of Taiwan under the Projects Nos. NSC96-2218-E-019-003 and APORC-95C100303. The support of the ARL:UT team providing the acoustic source transmissions and the R/V KNORR crew is appreciated.

References and links

[1]P. Gerstoft and D. F. Gingras, "Parameter estimation using multifrequency range-dependent acoustic data in shallow water," J. Acoust. Soc. Am. **99**, 2839–2850 (1996).
[2]M. Siderius, P. L. Nielsen, J. Sellschopp, M. Snellen, and D. Simons, "Experimental study of geo-acoustic inversion uncertainty due to ocean sound-speed fluctuations," J. Acoust. Soc. Am. **110**, 769–781 (2001).
[3]Y.-T. Lin, C.-F. Chen, and J. F. Lynch, "An equivalent transform method for evaluating the effect of water-column mismatch on geoacoustic inversion," IEEE J. Ocean. Eng. **31**, 284–298 (2006).
[4]C. F. Huang, P. Gerstoft, and W. S. Hodgkiss, "On the effect error correlation on matched-field geoacoustic inversion," J. Acoust. Soc. Am. **121**(2), EL64–EL69 (2007).
[5]Y.-M. Jiang and N. R. Chapman, "Bayesian geoacoustic inversion in a range dependent shallow water environment," J. Acoust. Soc. Am. **123**(6), EL155–EL161 (2008).
[6]A. Turgut, "SW06 bottom characterization by using chirp sonar and GeoProbe data," in *Shallow Water 2006 Experiment San Diego Workshop* (2007).
[7]W. M. Carey, J. Doutt, R. B. Evans, and L. M. Dillman, "Shallow-water sound transmission measurements on the New Jersey continental shelf," IEEE J. Ocean. Eng. **20**, 321–336 (1995).
[8]P. Gerstoft, SAGA Users guide 5.0, an inversion software package. An updated version of "SAGA 2.0," SACLANT Undersea Research Centre, SM-333, La Spezia, Italy (1997).
[9]S. E. Dosso, "Quantifying uncertainty in geoacoustic inversion I: A fast Gibbs sampler approach," J. Acoust. Soc. Am. **111**, 129–142 (2002).
[10]Y.-M. Jiang, N. R. Chapman, and M. Badiey, "Quantifying the uncertainty of geoacoustic parameter estimates for the New Jersey shelf by inverting air gun data," J. Acoust. Soc. Am. **121**, 1879–1894 (2007).